

# Dihexylquaterthiophene, A Two-Dimensional Liquid Crystal-like Organic Semiconductor with High Transport Properties<sup>†</sup>

F. Garnier,<sup>\*,‡</sup> R. Hajlaoui,<sup>‡</sup> A. El Kassmi,<sup>‡</sup> G. Horowitz,<sup>‡</sup> L. Laigre,<sup>‡</sup> W. Porzio,<sup>§</sup> M. Armanini,<sup>§</sup> and F. Provasoli<sup>§</sup>

Laboratoire des Matériaux Moléculaires, CNRS, rue Dunant 94320, Thiais, France, and Istituto di Chimica delle Macromolecole del C.N.R., via E. Bassini, 20133 Milano, Italy

Received October 30, 1997. Revised Manuscript Received June 4, 1998

End-substitution of quaterthiophene with hexyl groups leads to a highly soluble conjugated oligomer,  $\alpha,\omega$ -dihexylquaterthiophene (DH4T), which has been characterized for its thermal, structural, and electrical properties. Differential scanning calorimetry indicates the existence of a 3-dimension (3D)-to-mesophase transition, occurring at 84 °C, below the melting temperature of the material (179 °C). X-ray diffraction patterns performed on crude and thermally treated films of DH4T confirm the existence of a smectic phase with two spacings that increase with temperature. This result is interpreted by a model involving alkyl chain movements, which result in spacing shrinkage, whereas the thienylene sequence remains faced at typical van der Waals distances. DH4T thus forms a 2-dimensional (2D) semiconductor with a liquid crystal-like structural organization. DH4T can be deposited as active semiconducting layer in thin-film transistors, either by vacuum evaporation or by spin coating on an octylsilane-pretreated surface. A high-field-effect carrier mobility has been obtained for both deposition techniques,  $\mu = 3 \times 10^{-2}$  and  $1.2 \times 10^{-2}$  cm<sup>2</sup> V<sup>-1</sup> s<sup>-1</sup>, respectively, together with an interesting  $I_{on}/I_{off}$  ratio of 10<sup>5</sup>. These data are discussed together with literature results on unsubstituted quaterthiophene (4T) and the parent sexithiophenes (DH6T and 6T). On one hand, results show that the semiconducting quaterthiophene core in DH4T is large enough to allow high charge transport properties, comparable to those of a sexithiophene core, whereas the core is also short enough to allow its  $\alpha,\omega$ -dialkylated derivative to be highly soluble and solution processable, contrary to the case of DH6T. Results also suggest that the larger band gap of the shorter conjugated quaterthiophenes is responsible for their lower dopant concentration, and hence of their higher dynamic ratio.

## Introduction

Organic semiconductors have been studied since the early 1950s, and the large amount of work devoted to them allowed a better understanding of their charge transport properties. However, because of their very poor semiconducting characteristics, they were merely considered as exotic materials with little potential interest for applications until the late 1980s, when two significant steps simultaneously appeared in the literature; that is, light-emitting diodes could be made from a conjugated semiconducting polymer,<sup>1</sup> and efficient field-effect transistors (FET) could be realized from short conjugated oligomers.<sup>2</sup> These two results launched intensive research on these two types of organic-based

devices, and the extensive work accomplished since has largely confirmed the technological pertinence of organic semiconductors, showing the promise for applications in flexible and large area electronics. Two categories of organic semiconductors are actually under development: conjugated polymer-based ones, whose amorphous state is favorable to strong luminescence, and conjugated oligomer-based ones, in which it has been demonstrated that the efficiency of charge transport is directly related to the long-range packing of molecules in the semiconducting film. In fact, conjugated oligomers can be considered as forming molecular (poly)-crystals, whose electrical properties are essentially controlled by molecular order. Thus, performances of FET based on sexithiophene (6T) have been improved by a factor of nearly 50 by controlling the molecular ordering in the evaporated film, from a short-range ordered 3-dimensional (3D) structure to a well-organized 2-dimensional (2D) arrangement, where the molecules tend to stack along a packing axis nearly parallel to the substrate surface.<sup>3</sup> This approach, first demonstrated

\* Author to whom correspondence should be addressed.

<sup>†</sup> Presented at the 1997 Materials Research Society Spring Meeting, San Francisco, CA, April, 1997.

<sup>‡</sup> Laboratoire des Matériaux Moléculaires.

<sup>§</sup> Istituto di Chimica delle Macromolecole del C.N.R.

(1) Burroughes, J. H.; Bradley, D. D. C.; Brown, A. R.; Marks, R. N.; Mackay, K.; Friend, R. H.; Burn, P. L.; Holme, A. B. *Nature* **1990**, *347*, 539.

(2) Horowitz, G.; Fichou, D.; Peng, X. Z.; Xu, Z.; Garnier, F. *Solid State Comm.* **1989**, *72*, 381; Garnier, F.; Horowitz, G.; Peng, X. Z.; Fichou, D. *Adv. Mater.* **1990**, *2*, 592.

(3) Servet, B.; Horowitz, G.; Ries, S.; Lagorse, O.; Alnot, P.; Yassar, A.; Deloffre, F.; Srivastava, P.; Hajlaoui, P.; Lang, P.; Garnier, F. *Chem. Mater.* **1994**, *6*, 1809.

on oligothiophenes, has been recently confirmed in the case of pentacene.<sup>4a,b</sup>

Long-range order in films of molecular materials can be achieved by controlling the experimental conditions for film deposition, such as the substrate temperature and the rate of evaporation, which allowed achievement of mobility of  $2 \times 10^{-2} \text{ cm}^2 \text{ V}^{-1} \text{ s}^{-1}$  in 6T. But an elegant and efficient chemical route has also been proposed for inducing long-range order, based on the grafting of alkyl groups at both ends of the molecule (e.g., in  $\alpha,\omega$ -dihexylsexithiophene, DH6T). Alkyl groups are known to bring mesogenic properties, which explains the higher field-effect mobility of DH6T, which is around  $10^{-1} \text{ cm}^2 \text{ V}^{-1} \text{ s}^{-1}$ .<sup>5</sup> Transistors have been also realized from single crystals of oligothiophene, which showed mobility values (about  $2 \times 10^{-1} \text{ cm}^2 \text{ V}^{-1} \text{ s}^{-1}$ ) only slightly higher than that observed in the latter, highly ordered films.<sup>6</sup> These results suggest that the field effect mobilities actually obtained with ordered oligomer films, either oligothiophenes or oligacenes, almost reached the limit that can be expected for perfectly ordered crystalline materials. Such a limit can be set to about 1 to 5  $\text{cm}^2 \text{ V}^{-1} \text{ s}^{-1}$ , as deduced from careful time-of-flight mobility measurements carried out on single crystals of condensed aromatic hydrocarbons.<sup>7</sup>

These considerations raise the question about the problems that now have to be faced for improving organic semiconductor-based devices. Among them, one can consider the lack of solution processability of oligomer-based semiconductors, which does not yet allow the full use of the advantages expected from organic materials, and the problem raised by the fairly low dynamic ratio (i.e.,  $I_{\text{on}}/I_{\text{off}}$  ratio) as measured at relevant voltages applied to the transistor electrodes (i.e., some few volts). With the aim to answer these questions, we report here the structural and electrical properties of a short conjugated oligothiophene, quaterthiophene 4T, on which two hexyl groups have been substituted on its end position; that is,  $\alpha,\omega$ -dihexylquaterthiophene (DH4T).

## Experimental Section

Quaterthiophene, 4T, has been synthesized by a classical lithiation of bithiophene (Aldrich) using *n*-butyllithium in anhydrous tetrahydrofuran (THF) at  $-70^\circ \text{C}$ , followed by a coupling involving 2 M equivalent anhydrous copper (II) chloride. The solution was slowly warmed to room temperature, and maintained under stirring for 12 h. Water was then added under acidic pH, leading to a precipitate that was purified on a Soxhlet with  $\text{CH}_2\text{Cl}_2$ . 4T appeared as a yellow polycrystalline powder, whose structure was confirmed by  $^1\text{H}$  and  $^{13}\text{C}$  NMR and mass spectrometry.

Synthesis of DH4T involved first the coupling of 2-bromothiophene (Aldrich) and 2-hexylthiophene (Lancaster). 2-Hexylthiophene was lithiated with *n*-butyllithium and tetramethylenediamine in anhydrous THF at  $-70^\circ \text{C}$ . The resulting solution was stirred for 30 min and then allowed to

warm to room temperature. A molecular equivalent solution of zinc chloride in anhydrous diethyl ether was then added in a dropwise manner and, after 1 h, an equivalent amount of 2-bromothiophene was added, and the adduct was stirred for 20 h. The resulting reaction mixture was hydrolyzed under acidic pH, and the organic layer was extracted with diethyl ether and washed with water. A first purification step was performed by Soxhlet extraction, followed by purification using column chromatography on  $\text{SiO}_2$ , with 98:2 heptane:ethyl acetate eluant. This purification afforded 2,2'-(bithien-yl)-hexane, which was characterized by  $^1\text{H}$  and  $^{13}\text{C}$  NMR and by mass spectroscopy. The coupling of this latter compound was realized by a first lithiation using *n*-butyllithium in anhydrous THF at  $-70^\circ \text{C}$ , followed by the addition of 2 M equivalent of anhydrous copper chloride. After hydrolysis under acidic conditions and purification on a Soxhlet with  $\text{CH}_2\text{Cl}_2$ , a yellow-brown compound was obtained (DH4T) whose structure was confirmed by  $^1\text{H}$  and  $^{13}\text{C}$  NMR and by mass spectroscopy. One important property of DH4T is its extremely high solubility in chlorinated solvent, such as dichloromethane or chloroform, which reaches the range of  $\text{M L}^{-1}$  and makes this compound compatible with the spin-coating process.

The differential scanning calorimetry (DSC) measurements were carried out using a Perkin-Elmer DSC Pyris apparatus under nitrogen flux. X-ray diffraction (XRD) experiments were performed with a Siemens D-500 computer-controlled apparatus, with Soller slits ( $2^\circ$  divergence), graphite-monochromator (002 direction) after the sample, using  $\text{CuK}\alpha$  radiation.

The electrical properties were determined with a thin-film transistor (THF) structure following an already described procedure.<sup>2</sup> The realization of the TFT involved two types of structures. One type was a highly doped silicon substrate that formed the gate electrode, on which a thin film of silicon oxide ( $\text{SiO}_2$ ) was thermally grown for realizing the insulating layer, with a thickness of about  $0.3 \mu\text{m}$ . The other type was a glass substrate on which an aluminum stripe was first evaporated as gate electrode, followed by the spin coating of a thin layer of poly(methyl methacrylate) (PMMA), with a thickness of about  $0.5 \mu\text{m}$ , forming the insulating layer. A thin film of the semiconducting oligomer was then deposited, either by vacuum evaporation or by spin coating, with a thickness of about 50 nm. Deposition of DH4T on  $\text{SiO}_2$  by spin coating first required chemical modification of the  $\text{SiO}_2$  surface to make it organic compatible. The  $\text{SiO}_2$  surface was first cleaned, dried, and immersed in a  $10^{-2} \text{ M}$  chloroform solution of trichloro *n*-octylsilane, which is known to lead to the formation of a self-assembled monolayer of *n*-octylsilane on the  $\text{SiO}_2$  surface. The presence of an *n*-octyl layer onto the  $\text{SiO}_2$  surface appeared to be essential for the formation of a polycrystalline film of DH4T, obtained by spin coating of a  $6 \times 10^{-2} \text{ M}$  chloroform solution on a substrate held at  $110^\circ \text{C}$ . Two source and drain electrodes were then vacuum evaporated, affording a channel length of  $50 \mu\text{m}$  and a channel width of 5 mm. The electrical characterizations were carried out in an electrically shielded box, using a computer-monitored picoameter/dc source (Hewlett-Packard 4140B).

## Results

**Thermal Properties.** The thermal properties of DH4T are reported in Figure 1, where successive DSC scans are displayed. The first heating run clearly shows a first endothermic peak centered at  $84^\circ \text{C}$  ( $\Delta H = 0.076 \text{ J/mol}$ ), which is attributable to a transition from a 3D organization to a mesophase, followed by a second endothermic peak at  $179^\circ \text{C}$  ( $\Delta H = 0.149 \text{ J/mol}$ ), which is due to melting of the material. In the second scan (i.e., cooling), two exothermic peaks are present at  $176$  and  $57^\circ \text{C}$ , which can be assigned to mesophase and 3D crystallizations, respectively, and whose  $\Delta H$ s are in the same ratio as are the endothermic ones, although they result in smaller energy levels, probably because of

(4) (a) Grundlach, J. D.; Lin, Y. Y.; Jackson, T. N.; Nelson, S. F.; Schlom, D. G. *IEEE Electron Device Lett.* **1997**, *18*, 87. (b) Katz, H. E.; Lovinger, A. J.; Dodabalapur, A. *Chem. Mater.* **1996**, *8*, 2542.

(5) Garnier, F.; Yassar, A.; Hajlaoui, R.; Horowitz, G.; Deloffre, F.; Servet, B.; Ries, S.; Alnot, P. *J. Am. Chem. Soc.* **1993**, *115*, 8716; Dimitrakopoulos, C. D.; Furman, E. K.; Graham, F.; Hedge, S.; Purushothaman, S. *Synth. Met.* **1998**, *92*, 47.

(6) Horowitz, G.; Garnier, F.; Hajlaoui, R.; Kouki, F. *Adv. Mater.* **1996**, *8*, 52.

(7) Pope, M.; Swenberg, C. E. *Electronic Processes in Organic Crystals*; Oxford University: New York, 1982.

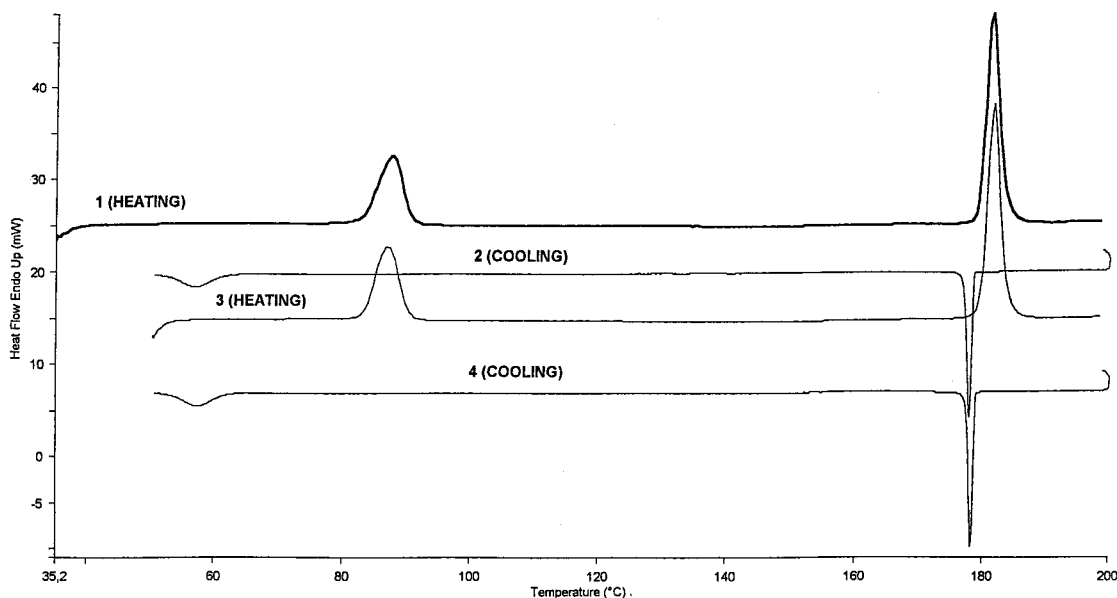


**Figure 1.** DSC curves of DH4T both on heating (runs 1 and 3) and on cooling (runs 2 and 4).

incomplete crystallization. The third and fourth scans carefully map the previous ones. In fact, the difference in energy involved is within the experimental errors, therefore indicating the absence of any hysteresis, that is, complete reversibility of the phenomena.

**X-ray Diffraction.** X-ray diffraction analysis was performed on both crude (A) and thermally treated (B) samples. In Figure 2, the patterns of both A and B are reported. The lamellar morphology of the crystal, observable by optical microscopy, results in a strong preferred orientation in spectrum A, where the most intense effects are different orders of the same crystallographic direction ( $d = 28.5 \text{ \AA}$ ). On the basis of the structural determinations of thienylenic oligomers,<sup>8,9</sup> it is reasonable to assume that this axis is the long unit cell edge, the mean molecular axis being closely aligned along this edge. In fact, molecular mechanics calculations using Hyper Chem program<sup>10</sup> show that the length of the molecule in extended conformation is about  $32 \text{ \AA}$ , van der Waals interactions being taken into account. Hence, the angle between these two directions is derived to be about  $25^\circ$ .

By using TREOR program,<sup>11</sup> we could index the spectrum, assuming an orthorhombic symmetry. The derived unit cell together with the  $d$  spacings of pristine and  $90^\circ \text{C}$  heated samples are reported in Table 1. The long spacing shrinkage above the first endothermic transition ( $d = 26.5 \text{ \AA}$ ) can be attributed to alkyl side chain rotations; that is, from an extended chain trans conformation to skew/gauche conformation.

Concerning the other  $d$  spacings, it should be noted that the transition to mesophase (according to DSC data) results in the disappearance of all XRD midrange effects. The remaining quite weak effects are either orders of main spacing or spacings observed in the 3D phase, except for a peak at  $3.8 \text{ \AA}$ .

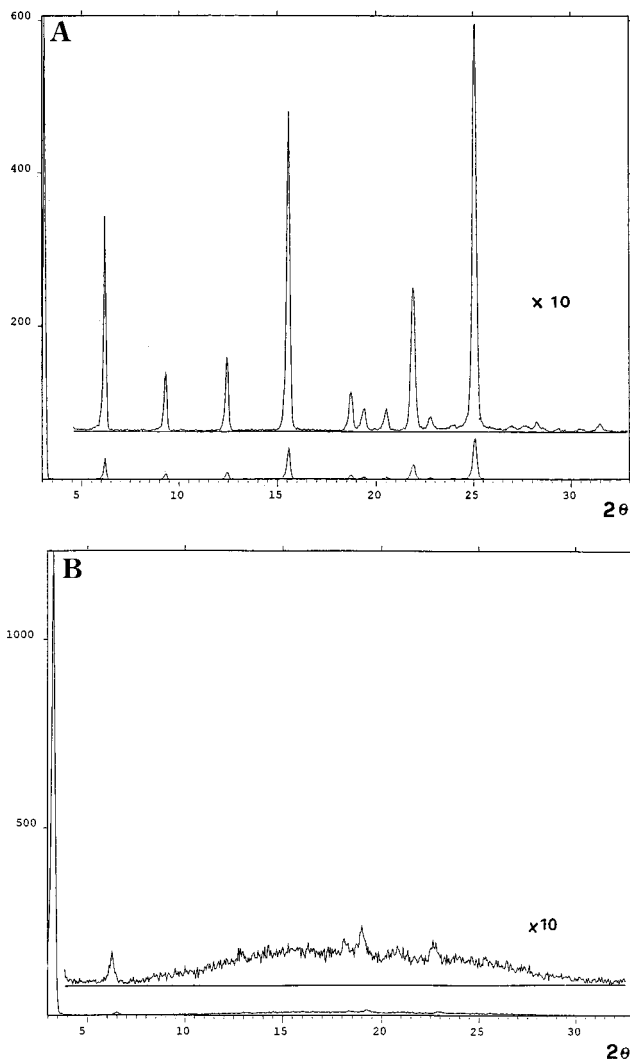


**Figure 2.** XRD patterns of (A) crude and (B) thermally treated, at  $90^\circ \text{C}$ , DH4T samples.

The spectrum at  $140^\circ \text{C}$  is quite similar to that at  $90^\circ \text{C}$  with increased  $d$  spacings; as matter of fact, the main peak is shifted to  $27 \text{ \AA}$  and the midrange one is shifted

(8) Porzio, W.; Destri, S.; Mascherpa, M.; Brückner, S. *Acta Polym.* **1993**, *44*, 266.

(9) Hotta, S.; Waragai, K. *Adv. Mater.* **1993**, *5*, 896.

(10) *Hyperchem Release 2.0 for Windows*; Hypercube Inc., and Autodesk Inc., CA, 1991.

(11) Werner, P. E.; Eriksson, L.; Westdahl, M. *J. Appl. Crystallogr.* **1985**, *18*, 367.

**Table 1. Unit Cell Parameters, Assuming Orthorhombic Symmetry, and  $d$ -Spacings of the Molecules at 25 and 90 °C<sup>a</sup>**

$hkl$	$d$ (25 °C)	$d$ (90 °C)
100	28.4	26.85
200	14.2	13.42
300	9.48	
400	7.10	6.71
500	5.68	
600	4.73	4.5
220	4.58	
002	4.45	
102	4.40	
320	4.32	
700	4.06	
212	3.90	3.8
312 <sup>b</sup>	3.71	
800	3.55	
801	3.30	
030	3.22	
621	3.16	
330	3.04	
131 <sup>b</sup>	3.01	
721 <sup>b</sup>	2.93	
1000	2.84	

<sup>a</sup>  $a = 28.4$  Å,  $b = 9.67$  Å,  $c = 8.90$  Å,  $d_{\text{calc}} = 1.35$  g cm<sup>-3</sup>,  $d_{\text{exp}} = 1.33$  g cm<sup>-3</sup>. <sup>b</sup> Indicates weak and broad peaks.

to 3.87 Å. The spectrum at 180 °C is completely amorphous, in agreement with a liquid phase. The XRD spectra recorded at room temperature after such a temperature cycle is essentially equivalent to the pristine one, aside from some peak broadening due to incomplete crystallization, which is in agreement with the DSC cooling runs. These observations are fully consistent with DSC data, and reveal the existence of a smectic phase with two spacings increasing with temperature. This fact is also in agreement with the model assumed in which the alkyl chain movements result in long spacing shrinkage, whereas the thienylene sequences remain faced at typical van der Waals distances.<sup>12</sup> When the temperature is increased, the energy of molecules becomes high enough to allow significant deviations from planarity in the thienylene sequences, which leads to the enlargement of both long and short spacings.

We like to observe that line profile analysis,<sup>12</sup> performed on the mesophase XRD spectrum at 90 °C, indicates a crystallite size >250 Å, along the main axis (i.e., about 9 unit cells) and a larger dimension of 400 Å along the thienyl-facing direction, corresponding to a coherence of >100 unit cells.

**Electrical Properties.** The electrical properties of this alkylated quaterthiophene can be expected to be largely dominated by such long-range 2D organization. We will consider in the following the carrier mobility of DH4T, as determined from TFT characteristics, and compare it with that of unsubstituted quaterthiophene 4T, and discuss these data together with results already obtained on the parent sexithiophene 6T and its dihexyl-substituted derivative DH6T.

Thin-film transistors fabricated from 4T and DH4T show remarkable amplification characteristics (Figure 3), with very well-defined linear and saturation regimes. The fact that current amplification appears at negative

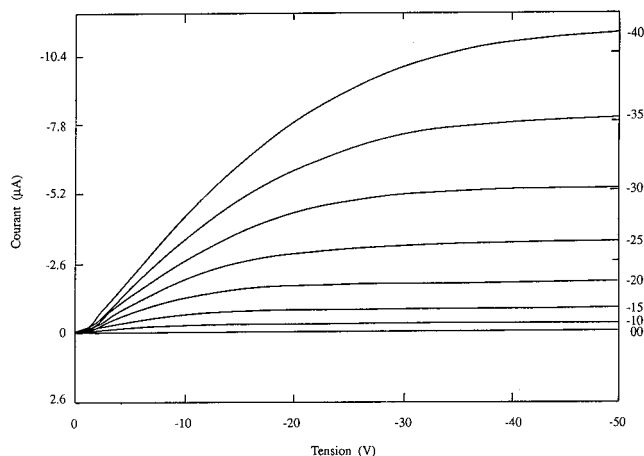


**Figure 3.** Drain current versus drain voltage characteristics for different source-gate voltages of a TFT based on a DH4T semiconducting layer vacuum evaporated on a PMMA insulating layer, with 2 nF cm<sup>-2</sup> capacitance (device channel length = 50 µm, channel width = 5 mm).

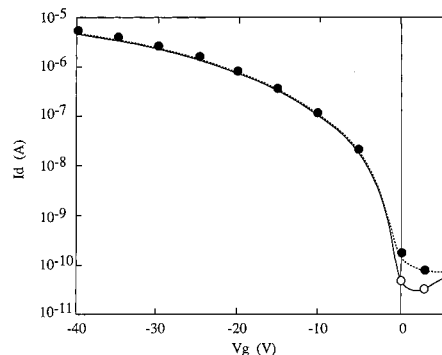


**Figure 4.** Transfer curve of DH4T-based TFT. Plot of drain current,  $I_d$ , versus source-gate voltage,  $V_g$ , in both directions at constant drain bias  $V_d$  of -30 V.

drain and gate voltages is typical of a  $p$ -type semiconducting material. The field-effect mobility,  $\mu_{\text{FE}}$ , was calculated from both linear and saturation current regimes with classical eqs 1 and 2, respectively

$$g_m = (dI_d/dV_g) V_d = (W/L) C_i \mu_{\text{FE}} V_d \quad (1)$$

$$I_{d,\text{sat}} = (W/2L) C_i \mu_{\text{FE}} (V_g - V_T)^2 \quad (2)$$

where  $I_d$  is the observed drain current,  $V_g$  is the gate voltage,  $V_d$  is the drain voltage,  $W$  and  $L$  are the channel width and length, respectively,  $C_i$  is the dielectric capacitance per unit area,  $\mu_{\text{FE}}$  is the field-effect mobility,  $V_T$  is the threshold voltage,  $g_m$  is the transconductance, and  $I_{d,\text{sat}}$  is the drain current at saturation. The field-effect mobilities have been calculated in the linear regime at a low drain voltage,  $V_d = -2$  V, and the dynamic ratio,  $I_{\text{on}}/I_{\text{off}}$ , at a drain voltage of  $V_d = -30$  V. Because of the  $p$ -type character of the semiconducting oligothiophenes, these organic-based transistors operate in the classical accumulation regime under negative gate bias, and also under depletion regime under positive gate bias, up to complete depletion of the semiconducting layer, which is associated to the lowest observed current,  $I_{\text{off}}$ . The transfer curve,  $I_d = f(V_g)$  at constant drain voltage, Figure 4, allows one to calculate the dynamic ratio of the device (i.e.,  $I_{\text{on}}/I_{\text{off}}$ ), which is

(12) See e.g., Bolognesi, A.; Porzio, W.; Zhuo, G.; Ezquerro, T. *Eur. Pol. J.* **1996**, *32*, 1097 and references therein.

**Table 2. Field-Effect Mobility,  $\mu_{FE}$ , Dynamic Ratio,  $I_{on}/I_{off}$ , and Depletion Pinch-Off Voltage,  $V_p$ , in TFTs Based on Sexithiophene and Quaterthiophene Derivatives**

oligothiophene	mobility, $\mu$ ( $\text{cm}^2 \text{V}^{-1} \text{s}^{-1}$ ) <sup>a</sup>	$I_{on}/I_{off}$ <sup>b</sup>	depletion pinch-off, voltage, $V_p$ (V)
sexithiophene, 6T <sup>c</sup>	$2 \times 10^{-2}$	$2 \times 10^4$	-20
$\alpha,\omega$ -dihexylsexithiophene, DH6T <sup>b</sup>	$8 \times 10^{-2}$	$10^4$	-25
quaterthiophene, 4T	$2.5 \times 10^{-3}$	$8 \times 10^4$	-5
$\alpha,\omega$ -dihexylquaterthiophene, DH4T (vacuum evaporated)	$3 \times 10^{-2}$	$10^5$	-2
$\alpha,\omega$ -dihexylquaterthiophene, DH4T (spin coated)	$1.2 \times 10^{-2}$	$3 \times 10^4$	-5

<sup>a</sup> Measured at drain voltage  $V_d = -2$  V. <sup>b</sup> Approximate value calculated from data obtained with a drain voltage  $V_d = -30$  V and for gate voltage  $V_g$  varying between +10 and -30 V. <sup>c</sup> Taken from ref 3.

also a critical parameter of a TFT. Care has been taken to calculate this parameter with low voltages; that is, -30 V for the drain voltage, and +10 to -30 V for the gate voltage range. These data are presented in Table 2 together with values previously obtained with sexithiophene derivatives, which will be used for comparison. The reproducibility of the measured values was within  $\pm 10\%$ , and these devices did not show appreciable variation of their characteristics with time.

The most significant results concern the high carrier mobility of DH4T, which appears close to that of the longer oligomer DH6T; the very close mobility value observed for spin-coated and vacuum-evaporated DH4T; and the much larger dynamic ratio observed for DH4T than for DH6T. These electrical properties will be discussed in terms of the *field-effect mobility* and the *dynamic ratio*.

### Discussion

Results show first that 4T possesses a much higher mobility than assessed in previous literature data. Previous publications both from the CNRS group as well as others have already suggested that sexithiophene, 6T, presents a charge carrier mobility of about  $2 \times 10^{-2} \text{ cm}^2 \text{ V}^{-1} \text{ s}^{-1}$ ,<sup>2,3,6,13</sup> but mobilities of the order of  $10^{-7} \text{ cm}^2 \text{ V}^{-1} \text{ s}^{-1}$  for 4T.<sup>14,15</sup> This behavior was at variance with what has been observed for a long time on another deeply studied family of molecular crystals, the polyacenes, where time-of-flight mobility at room temperature is in the range  $0.1$  to  $1 \text{ cm}^2 \text{ V}^{-1} \text{ s}^{-1}$ , whatever the length of the molecule, from naphthalene to tetracene.<sup>7</sup> Later, much higher values of the order of  $10^{-3} \text{ cm}^2 \text{ V}^{-1} \text{ s}^{-1}$  were reported for 4T, and the results obtained here,  $\mu = 2 \times 10^{-3} \text{ cm}^2 \text{ V}^{-1} \text{ s}^{-1}$ , indicate a slight decrease of its carrier mobility compared with that of 6T, and appear more reasonable when taking into account literature results on charge transport in molecular materials. It must be also mentioned that this value has been obtained for an oligomer film deposited on a substrate held at room temperature. The discrepancy of literature results on 4T could be due to the higher purity of this semiconducting material used in the present work, which has been subject to a first sublimation as purification procedure. The much lower concentration of structural defects and chemical impurities associated with higher purity can be thought to favor a long-range molecular organization of 4T in the film, and

also to minimize the occurrence of traps for the injected charges. The existence of a well-organized thin film of 4T can be further confirmed by measuring the ultraviolet (UV)-visible (vis) absorption under polarized light, the measurements being performed under an incidence angle of  $60^\circ$ . The *s*-polarized light has its polarization vector perpendicular to the incidence plane, thus parallel to the film surface, whereas the *p*-polarized light has its polarization vector parallel to the plane of incidence, hence partly parallel and partly perpendicular to the film surface. 4T possess an absorption band located around 3.6 eV in the solid state that is associated with an electronic transition polarized along the long axis of the molecules. It can be expected that if the 4T molecules are well ordered within the film, a dichroic ratio should be observed in the absorption spectra recorded respectively under *s*- and *p*-polarized light. This feature is indeed observed in films of 4T, and the dichroic ratio of about 2 in favor of the *p*-polarized light indicates that the 4T molecules are oriented predominantly perpendicular to the film surface,<sup>16,17</sup> as already observed for films of sexithiophene.<sup>3,5</sup>

When comparing unsubstituted with dihexyl-substituted materials, results show that the ratio of mobilities is larger for 4T than for 6T derivatives, with values of 12 and 4, respectively. This larger ratio for the shorter oligomer can be attributed to the larger contribution of the hexyl group to the whole molecule DH4T, as compared with DH6T, which is expected to enhance its mesogenic properties for the induction of long-range molecular organization. Thus, as clearly demonstrated already by results based on differential calorimetry and X-ray structural characterizations, DH4T readily forms a 2D semiconductor with a liquid crystal organization. Such long-range orientation has already been demonstrated to be the key for a highly efficient charge transport within a material. The value of mobility obtained for DH4T, in the range of  $1.2 \times 10^{-2}$  to  $3 \times 10^{-2} \text{ cm}^2 \text{ V}^{-1} \text{ s}^{-1}$ , associated with its extremely high solubility make this material of particular interest for potential applications for organic-based devices.

The dynamic ratio,  $I_{on}/I_{off}$ , also forms a major criterion required when discussing the relevance of a thin-film transistor. This value is obtained by plotting the transfer curve [i.e.,  $I_d = f(V_g)$ ] at constant  $V_d$ , as shown in Figure 4. It must be also underlined that a complete cycle in  $V_g$  values (i.e.,  $+V_g/-V_g/+V_g$ ) must be carried

(13) Dodabalapur, A.; Torsi, L.; Katz, H. E. *Science* **1995**, *268*, 270.

(14) Horowitz, G.; Peng, X. Z.; Fichou, D.; Garnier, F. *Synth. Met.* **1992**, *51*, 419.

(15) Akamichi, H.; Waragai, K.; Hotta, S.; Kano, H.; Sakati, H. *Appl. Phys. Lett.* **1991**, *58*, 1500.

(16) Egelhaaf, H. J.; Bäuerle, P.; Rauer, K.; Hoffmann, V.; Oelkrug, D. *J. Mol. Struct.* **1993**, *293*, 249.

(17) Hajlaoui, R.; Horowitz, G.; Garnier, F.; Arce-Brouchet, A.; Laigre, L.; El Kassmi, A.; Demanze, F.; Kouki, F. *Adv. Mater.* **1997**, *9*, 389.

out to check for the absence of any hysteresis, which would strongly question the relevance of such device. Comparable results are obtained for DH4T-based TFTs, realized either by vacuum deposition or by spin coating of the semiconductor. When analyzing data that have been reported in the literature on the dynamic ratio of organic-based TFTs, one can feel confused by the diversity of experimental conditions used for measuring this value.

The importance of the dynamic ratio of a TFT justifies some basic comments about the real meaning of literature data. As a matter of fact, TFTs that are used in practical applications, such as in flat panel displays, operate in a low potential range, between 0 and about 10–20 V for the gate voltage  $V_g$ , and with a low drain voltage,  $V_d$ , at most of about 10 V. Under these voltage conditions, the dynamic ratio measured for practical TFTs based on hydrogenated amorphous silicon is  $> 10^7$ . On the other hand, in most of literature data on organic-based devices, these potential ranges have been largely exceeded, up to about 100 V for  $V_d$  and  $\pm 100$  V for  $V_g$ , with the evident objective of reaching high values for the dynamic ratio. If values of some  $10^6$  have thus been quoted,<sup>4a</sup> their real meaning remains controversial, all the more because the field-effect mobility in these molecular materials appears to be field activated.

It must be thus remembered that the  $I_{on}$  value is directly determined by the carrier mobility of the semiconductor, as expressed in eq 2, and is also dependent on the value of the threshold voltage, which must be low enough to allow the term  $(V_g - V_T)$  to be as large as possible. Although several works have been carried out on organic-based devices, the parameters that control the threshold voltage  $V_T$  have not yet been clearly identified, so this material property will not be further discussed.

The event that determines the occurrence of the  $I_{off}$  regime in such a TFT is the complete depletion of the semiconducting layer, induced by a "pinch-off" gate voltage,  $V_p$ , given by eq 3

$$V_p = (qNd^2/2\epsilon_0\epsilon_s)(1 + 2C_s/C_i) \quad (3)$$

where  $N$  is the dopant concentration,  $d$  the thickness of the semiconducting layer, and  $C_s$  its dielectric constant. Equation 3 shows that the complete depletion voltage is dependent, among other variables, on the semiconductor film thickness,  $d$ , and also on the dopant concentration,  $N$ . TFTs that are actually considered as relevant in practical applications attain their  $I_{off}$  regime under low gate bias, close to 0 V. Hence, to reach operating conditions close to those required for real applications, it appears that organic-based TFTs should be constructed with a semiconducting layer as thin as possible, and also characterized by a very low dopant concentration. For technical reasons, thickness  $d$  has some lower limit, which can be estimated to tens of nanometers. On the other hand, the dopant concentration is an intrinsic material property, which can be varied by the proper choice of the semiconductor. Thus,

when passing from 6T to the lower conjugated 4T, the band gap energy increases from 2.25 to about 2.7 eV. Such an increase in  $E_g$  will be associated with a lowering of the valence band energy and hence, a decrease of the dopant concentration,  $N$ , which should lead on one hand to a pinch-off value  $V_p$  closer to 0 V, and on the other hand to a lower value of  $I_{off}$ .

In the present case, the results on the dynamic ratio measured with a polymer layer as insulator must be thus considered as largely underestimated values, in which  $I_{off}$  values are obscured by the presence of a leakage current, as shown in Figure 4 for positive gate bias. Taking this remark into account, the dynamic ratio obtained with DH4T, using a gate voltage range of +10 to -30 V and a constant drain potential of -30 V, is  $10^5$ , which can be considered as excellent compared with literature data. The absence of significant hysteresis when compared with literature data on other organic semiconductors<sup>16</sup> is also a point of interest. The data in Table 2 also clearly indicate that when passing from the long conjugated sexithiophene to the shorter conjugated quaterthiophene, a significant increase of the dynamic ratio is observed. This increase indicates that because of the higher band gap energy, quaterthiophene has a lower concentration of dopants (i.e., chemical species originating from the synthesized materials). This conclusion is further confirmed when analyzing the depletion pinch-off voltage,  $V_p$ , which is much closer to 0 V when passing from sexithiophene to quaterthiophene derivatives. Such a decrease of  $V_p$ , obtained for a same thickness of semiconducting layer in the TFTs, must be attributed to a lower dopant concentration in the material, as expected from eq 3.

In conclusion, shorter conjugated oligomers (e.g., quaterthiophenes), appear of high potential interest because the increase of the band gap energy ensures a large decrease in the dopant concentration. Following the equations describing the operating mode of TFTs, a low dopant concentration allows one to expect that the complete depletion of the semiconductor will occur at a potential near 0 V, and that the  $I_{off}$  current observed under these conditions will be very low; thus fulfilling the requirements for observing a large dynamic ratio. On the other hand, we have also shown how the alkyl-end-substitution on short oligomers (e.g., quaterthiophene) allows one to induce very high mesogenic properties for these materials, which are characterized by a liquid crystal transition and a highly ordered structure within the film. This organization leads to a high field-effect mobility of  $1.2 \times 10^{-2}$  to  $3 \times 10^{-2}$   $\text{cm}^2 \text{V}^{-1} \text{s}^{-1}$ . When taking also into account the very high solubility, which makes its solution processable, it appears that the alkyl-end-substitution on short conjugated oligomers is an interesting way toward producing efficient organic semiconductors.

**Acknowledgments.** Acknowledgments are made to Mr. Pascal Raynal, LMM-CNRS Thiays, for valuable experimental contribution to the synthesis of DH4T.

CM970704G